Annals of Nuclear Medicine Vol. 18, No. 6, 463–468, 2004

Evaluation of myocardial viability following acute myocardial infarction using ^{201}Tl SPECT after thallium-glucose-insulin infusion —Comparison with ^{18}F-FDG positron emission tomography—

Takuji TOYAMA,* Hiroshi HOSHIZAKI,* Ryotaro SEKI,* Naoki ISOBE,* Shigeru OSHIMA,* Koichi TANIGUCHI,* Kyosuke HIGUCHI,** Hidenori SEKI,** Takashi HATORI,** Masahiko KURABAYASHI** and Keigo ENDO**

Gunma Prefectural Cardiovascular Center
Gunma University School of Medicine

Objective and Methods: The aim of this study was to evaluate myocardial viability in patients after acute myocardial infarction (AMI). We compared ^{201}Tl SPECT after ^{201}Tl with GIK (10% glucose 250 m*l*, insulin 5 U and KCl 10 mEq) infusion (GIK-^{201}Tl) with resting ^{201}Tl and ^{99m}Tc-pyrophosphate (PYP) dual SPECT, positron emission computed tomography (PET) using ^{18}F-fluorodeoxyglucose (^{18}F-FDG) in 21 patients with their first AMI, who all underwent successful reperfusion. GIK-^{201}Tl SPECT, ^{201}Tl and ^{99m}Tc-PYP dual SPECT were done within 10 days after admission and ^{18}F-FDG-PET was performed at 3 weeks. GIK-^{201}Tl SPECT was obtained after 30 min of GIK-^{201}Tl infusion. ^{18}F-FDG (370 MBq) was injected intravenously after oral glucose (1 g/kg) loading, and then PET was obtained. PET and SPECT images were divided into 20 segments. Regional tracer uptake was scored using a 4-point scoring system (3 = normal to 0 = defect), and summed to a regional uptake score (RUS). Regional area means the infarcted area in which ^{99m}Tc-PYP accumulated. The number of decreased uptake segments (ES) was then determined. The infarcted area was defined as the area of ^{99m}Tc-PYP uptake. ***Results:*** The ESs for the GIK-^{201}Tl and ^{18}F-FDG-PET images were significantly lower than the number of ^{99m}Tc-PYP uptake segments. The RUS for GIK-^{201}Tl was higher than that for resting-^{201}Tl imaging and similar to those for ^{18}F-FDG-PET. ***Conclusions:*** In the detection of myocardial viability following AMI, GIK-^{201}Tl imaging is useful with findings similar to those of ^{18}F-FDG-PET.

Key words: GIK-^{201}Tl, stunned myocardium, acute myocardial infarction, ^{18}F-FDG-PET

INTRODUCTION

THE PROGNOSIS of patients with acute myocardial infarction (AMI) has improved with reperfusion therapy.[1–3] Even with successful reperfusion therapy, myocardium may be stunned and regional wall motion in the infarcted area is decreased.[4–6] In patients with AMI, it is clinically important to distinguish viable from nonviable myocardium to predict whether regional wall motion will eventually improve. Positron emission tomography (PET) is considered the gold standard for assessing myocardial viability, but alternative procedures based on radionuclide imaging have been proposed. ^{201}Tl myocardial scintigraphy has been widely used to detect myocardial viability based on late redistribution[7] or assessed using a reinjection imaging technique[8,9] in patients with coronary artery disease. A recent study by Tartagni[10] described a new method for cardiac imaging after infusion of ^{201}Tl, insulin, and potassium in a glucose solution, which improves the detection of viable myocardium. Insulin augments myocardial uptake of potassium through translocation of Na-K ATPase from the cytosol to the sarcolemma.[11,12] In a similar fashion, ^{201}Tl is taken up by

Received November 12, 2003, revision accepted April 13, 2004.

For reprint contact: Takuji Toyama, M.D., Gunma Prefectural Cardiovascular Center, 3–12 Kameizumi-machi, Maebashi, Gunma 371–0004, JAPAN.

E-mail: toyama.t@cvc.pref.gunma.jp

the myocardium via Na-K ATPase,[13,14] and its uptake is also enhanced by insulin. However, the effectiveness of ^{201}Tl imaging after the infusion of ^{201}Tl with glucose-insulin-potassium (GIK-^{201}Tl) has not been established, because there are no reports comparing the technique with ^{18}F-fluorodeoxyglucose (^{18}F-FDG)-PET, which is regarded as the gold standard to evaluate myocardial viability.

The aim of this study was to evaluate whether GIK-^{201}Tl can be used to detect myocardial viability in patients with AMI, comparing the technique with ^{18}F-FDG-PET.

MATERIALS AND METHODS

Patients

The study population comprised 21 patients (15 men, 6 women; 46 to 75 years of age, mean age: 62 ± 9 years) with initial AMI who had undergone successful percutaneous coronary intervention (PCI) with or without stenting within 6 h of the onset of symptoms. The diagnosis of AMI was based on the following criteria: acute chest pain lasting ≥ 30 min, serum creatine kinase activity over ≥ 500 IU, and the development of abnormal electrocardiographic Q waves.

Patients who fulfilled the following criteria were included in the statistical analysis: successful PCI with angiographic confirmation of ≤25% residual stenosis, no significant stenosis in other vessels, good image quality for all radiotracer studies during the subacute period and no restenosis based on coronary angiography (CAG) 3 weeks after admission. Patients with diabetes or glucose intolerance were excluded from the study. Glucose intolerance was defined as a fasting glucose concentration >110 mg/dl but <126 mg/dl, or a glucose concentration 2 h after a 75 g glucose load >140 mg/dl but <200 mg/dl. The infarct-related vessel was the left anterior descending coronary artery in 14 patients, the left circumflex artery in 3 patients, and the right coronary artery in 4 patients. Mean ejection fraction was 42 ± 10% based on left ventriculography (LVG) performed during the admission.

Study Protocol

The scintigraphic studies used were the resting ^{201}Tl and ^{99m}Tc-pyrophosphate (PYP) dual SPECT and ^{201}Tl SPECT after infusion ^{201}Tl with glucose-insulin-potassium (^{201}Tl-GIK SPECT), which were performed within 10 days after admission. ^{18}F-FDG-PET was performed 3 weeks after admission. All of the scintigraphic studies were performed after a 12-h overnight fast in the absence of antianginal medication. Coronary angiography (CAG) and LVG were performed within 3 weeks after admission.

All patients gave informed consent in accordance with the guidelines of our hospital's Human Clinical Study Committee prior to participation in the study.

Resting ^{201}Tl and ^{99m}Tc -PYP Dual SPECT

Each patient received 740 MBq of ^{99m}Tc-pyrophosphate intravenously and then 111 MBq of ^{201}Tl 2 hours later. Fifteen minutes after ^{201}Tl injection, all patients underwent myocardial imaging with dual SPECT.

Glucose-Insulin ^{201}Tl SPECT

Within 2 or 3 days after resting ^{201}Tl and ^{99m}Tc-PYP dual SPECT, ^{201}Tl-GIK SPECT was performed 15 min after a 30-minute infusion of 250 ml of 10% glucose plus insulin (5 U) and 10 mEq potassium chloride labeled with ^{201}Tl (111 MBq).[19] The infusion rate was adjusted using an automatic pump.

Myocardial SPECT Imaging

Myocardial SPECT imaging was performed using a PRISM3000 (PICKER, Cleveland, OH) three-headed SPECT system with low-energy, high-resolution, parallel-hole collimators. The detector system was interfaced to a dedicated nuclear medicine computer. A total of 60 projection images were obtained over a 360° arc in 6° increments, with 40 sec/view acquisitions for ^{201}Tl and GIK-^{201}Tl. The energy discriminator was centered on 72 keV for ^{201}Tl with a 30% window and 140 keV for ^{99m}Tc-PYP with a 15% window. The other energy discriminator was centered on 90 keV with 10% window for crosstalk correction.[15,16] The data were recorded in 128 × 128 matrices on a magnetic disk. To reconstruct transaxial tomographic images from each acquisition, Butterworth (order: 8, cutoff frequency: 0.15–0.17 cycle/pixel) and ramp filters were used. Short- and long-axis slices (3.2 mm thick), were generated. Subsequently, three serial slices (9.6 mm thick) of the SPECT images were added.

Myocardial PET Image

^{18}F-FDG (370 MBq) was injected intravenously 30 min after oral glucose (1 g/kg) loading. Fifty minutes later, PET scans were performed for 10 min per bed position. A dedicated PET camera (SET-2400W; Shimadzu Corporation, Kyoto, Japan) was used for FDG PET imaging. This camera has a 20 cm axial rectangular field of view (FOV) and a 59.5 cm transaxial FOV, and consists of 32 rings of 21, 504 bismuth germanate (BGO) crystals, giving 63 2D imaging planes. A coincidence time window of 15 ns was used. Position non-linearity and energy non-uniformity of the detector unit were corrected in real time. In the 2D mode, the axial coincidence path acceptance can be controlled from 1 to 8 detectors to optimize sensitivity and axial resolution. The system has 1 mm thick and 55 mm long content septa for the 2D mode. Sixty-three sinograms were stored in a large scale acquisition memory (1 GB) in the 2D mode. A dead time correction and physical decay correction for the radioisotope were performed in real time. A ^{68}Ge-^{68}Ga external rod source (185 MBq) rotated in a 640 mm radius to obtain blank scan and transmission scan data. Simultaneous transmission-

emission scans were performed in the SET-2400 PET scanner.[17]

Analysis of SPECT and PET Image

SPECT and PET analysis was based on one vertical long-axis slice and three short-axis slices for each study. In each patient, the corresponding vertical long- and short-axis tomograms from the ^{201}Tl, ^{201}Tl-GIK, ^{99m}Tc-PYP SPECT and ^{18}F-FDG-PET image sets were aligned. Additionally, one vertical long-axis slice and three short-axis views from the apical, middle, and basal ventricular levels were chosen for comparison. The vertical long-axis slice was used to evaluate the apical region, which was divided into two segments, while each short-axis slice was divided into six segments. Two experienced observers who were unaware of the patients' clinical history analyzed all SPECT and PET images. Semiquantitative visual analysis was performed by assigning regional tracer uptake activities using a four-point scoring system (uptake score): 0 = absent, 1 = severely reduced uptake, 2 = mildly reduced uptake, and 3 = normal uptake. Disagreements in interpretation were resolved by consensus. We defined the number of segments with reduced uptake (uptake score ≤ 2) as the extent score (ES), which was compared with the number of segments demonstrating ^{99m}Tc-PYP uptake. We defined the sum of the uptake scores in the infarcted area where ^{99m}Tc-PYP was accumulated as the regional uptake score (RUS). The ^{99m}Tc-PYP uptake segments were defined as the segments that could be visually confirmed.

Left Ventriculography

Left ventriculography was performed in the 30° right anterior oblique projection (RAO) with the patient in the supine position.

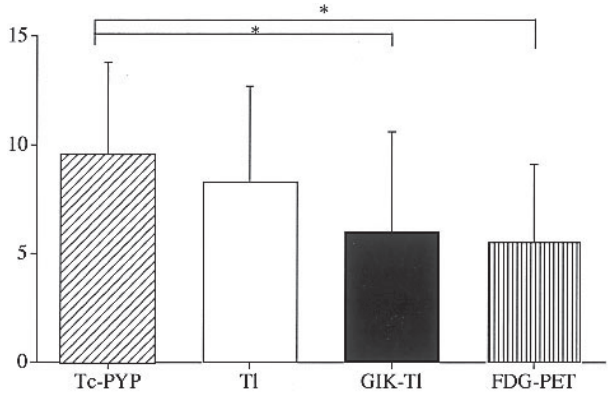

Fig. 1 Comparison of the number of ^{99m}Tc-PYP uptake segments and the extent scores using different imagings. *p < 0.05 vs. ^{99m}Tc-PYP imaging.

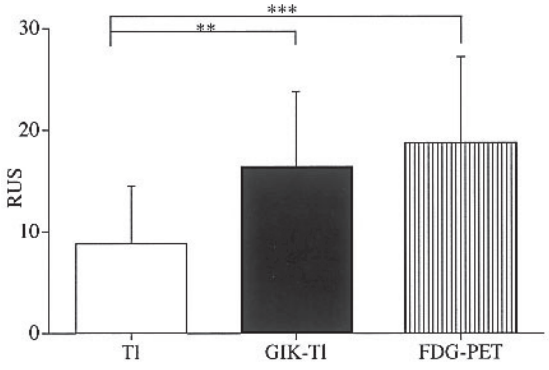

Fig. 2 Comparison of regional uptake scores using different imagings. **p < 0.01, ***p < 0.001 vs. resting ^{201}Tl imaging.

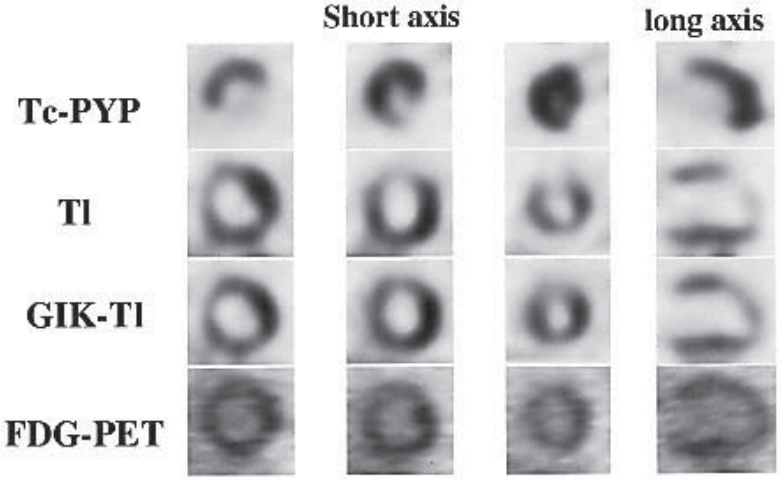

Fig. 3 This representative case illustrates an extensive anterior myocardial infarction in a 60-year-old man. ^{99m}Tc-PYP accumulated in the anteroseptal, anterior, and apical walls. Resting ^{201}Tl imaging showed accumulation in the anteroseptal wall, but defects in the anterior and apical walls. In contrast, GIK-^{201}Tl imaging showed accumulation not only in the anteroseptal but also the anterior and apical walls. These GIK-^{201}Tl images were similar to the ^{18}F-FDG-PET images.

Statistical Analysis

All data are presented as the mean ± SD. ANOVA was used to determine differences between values. A p value < 0.05 was considered statistically significant.

RESULTS

The extent scores for the different imagings modalities are shown in Figure 1. The number of ^{99m}Tc-PYP uptake segments and the extent scores for resting ^{201}Tl, GIK-^{201}Tl and ^{18}F-FDG-PET imagings were 9.6 ± 4.2, 8.3 ± 4.4, 6.0 ± 4.6 and 5.5 ± 3.6, respectively. The ES for GIK-^{201}Tl and ^{18}F-FDG-PET imagings were significantly lower than the number of ^{99m}Tc-PYP uptake segments.

The regional uptake scores for the different imaging modalities are shown in Figure 2. The regional uptake scores for resting ^{201}Tl, GIK-^{201}Tl and ^{18}F-FDG-PET images were 8.8 ± 5.7, 16.3 ± 7.5 and 18.8 ± 8.4, respectively. The values for GIK-^{201}Tl and ^{18}F-FDG-PET images were significantly higher than for resting ^{201}Tl imaging.

Figure 3 illustrates a representative case. A 60-year-old man with an acute anterior myocardial infarction, whose culprit lesion was the proximal left anterior descending artery, had successful reperfusion therapy 5 h after the onset of symptoms. The maximum CPK activity was 3145 IU/*l*.

DISCUSSION

Direct PCI is performed to treat acute myocardial infarction.[5,11,12] The success rate of reperfusion therapy is high, and the time to reperfusion is short, with a high degree of myocardial salvage. From the acute phase to the subacute phase, it is difficult to evaluate accurately the amount of myocardium that is salvaged because of stunning.[4–6]

The identification of salvaged myocardium was based on the overlap phenomenon using conventional dual ^{201}Tl and ^{99m}Tc-PYP SPECT images obtained during the acute phase of AMI.[18,19] In identifying the area of myocardial infarction, there is accumulation of ^{99m}Tc-PYP and decreased accumulation of ^{123}I-BMIPP and ^{123}I-MIBG, which are considered memory markers.[20–23] There is another method for assessing the infarcted area, based on identifying the area at risk. In this method, ^{99m}Tc-MIBI or ^{99m}Tc-tetrofosmin is injected just before reperfusion therapy[24] and SPECT imaging is obtained after reperfusion therapy. However, ^{201}Tl or ^{99m}Tc perfusion imagings underestimate the amount of salvaged myocardium because myocardial perfusion is improved on follow-up perfusion imaging.

Furthermore, myocardial contractile dysfunction in patients with AMI can be caused either by cellular necrosis or stunning. In contrast to necrotic tissue, stunned myocardium may recover. Therefore, it is clinically important to differentiate viable from necrotic myocardium.

Myocardial viability is determined by ^{18}F-FDG PET on the basis of preserved metabolic activity, irrespective of hypoperfusion or the presence of abnormal wall motion at rest. In patients with chronic coronary artery disease, a mismatch pattern between perfusion and ^{18}F-FDG images indicates the presence of ischemic or hibernating myocardium[23,24] with a high probability of recovery of contractile function after revascularization.[25,26] However, ^{18}F-FDG uptake does not always identify viable myocardium in patients with AMI because ^{18}F-FDG can gather in inflammatory cells in the infarcted area during the acute phase of AMI.[28–30] That is the reason why we obtained ^{18}F-FDG images 3 weeks after the onset of AMI.

Several studies have shown that insulin augments myocardial ^{201}Tl uptake.[10,31] Because of similarities between ^{201}Tl and potassium kinetics,[32,33] ^{201}Tl uptake may be affected by insulin administration. Insulin increases myocardial potassium turnover independent of metabolic changes.[34,35] This phenomenon may be exploited to detect hypoperfused but viable myocardium, because insulin administration before or during ^{201}Tl infusion promotes ^{201}Tl cellular uptake, especially in severely ischemic regions.[31] Insulin increases the membrane conductance of cations by activation of the Na K ATP-sensitive pump[36] with passive ^{201}Tl influx as a consequence of sodium efflux. This is the rationale behind the development of the GIK-^{201}Tl infusion method. GIK-^{201}Tl myocardial scintigraphy has been reported to be useful for evaluating hibernating myocardium after remote myocardial infarction.

In this study, we determined whether GIK-^{201}Tl myocardial scintigraphy could be used in the evaluation of salvaged myocardium after reperfusion, especially when compared with ^{18}F-FDG imaging. Based on the results of this study, the extent scores for GIK-^{201}Tl and ^{18}F-FDG PET imaging were smaller than the number of ^{99m}Tc-PYP imaging uptake segments. The regional uptake scores for GIK-^{201}Tl and ^{18}F-FDG PET were greater than the regional uptake score for resting ^{201}Tl imaging. Judging from the above results, resting ^{201}Tl imaging would underestimate the amount of salvaged myocardium. However, the extent and regional uptake scores for GIK-^{201}Tl imaging were similar to the extent and regional uptake scores for ^{18}F-FDG PET imaging. GIK-^{201}Tl imaging is useful in the evaluation of salvaged myocardium, specifically stunned myocardium in the subacute period of AMI.

In this study, patients with diabetes or glucose intolerance were excluded out of concern that the clinical data of these patients would affect the outcome. Of course, it is possible to perform FDG-PET using the insulin clamp method and GIK-^{201}Tl imaging by the adjustment of the insulin quantity in patients with diabetes or glucose intolerance.

Changes in plasma serum glucose, insulin and potassium concentrations could be problematic in this study. In

our prior study,[38] the plasma serum glucose, insulin and potassium were measured at the beginning and the end of GIK infusion. Insulin concentrations increased with insulin administration (7.1 ± 6.0 mU/m*l* at baseline versus 126 ± 88 mU/m*l* after GIK infusion; $p < 0.0005$). Serum glucose concentrations increased during GIK infusion, from 102 ± 16 mg/d*l* to 219 ± 40 mg/d*l*, and then rapidly decreased over the following 30 min to 126 ± 44 mg/d*l*. The potassium concentrations were not affected by this infusion (4.3 ± 0.4 mEq/*l* at baseline vs. 4.3 ± 0.4 mEq/*l* after GIK infusion). Based on these results, we determined that parenteral potassium chloride supplementation is safe.

Several limitations of this study should be considered. First, we obtained images following reperfusion therapy from a limited number of patients with AMI. Nonetheless, although our data need to be confirmed in a larger series, our findings strongly suggest that GIK-^{201}Tl imaging enhances the detection of viable myocardium after reperfusion. Secondly, because we have no follow-up data, we can not comment on the improvement in regional wall motion. Third, ^{18}F-FDG imaging was acquired 3 weeks after the onset of AMI, while SPECT imaging was performed earlier. ^{18}F-FDG imaging can not evaluate myocardial viability during the acute phase of AMI, because ^{18}F-FDG can accumulate in inflammatory cells in the infarcted area during that period.[37–39] However, stunned myocardium might recover to some extent during that time.

CONCLUSION

^{201}Tl imaging after GIK-^{201}Tl infusion is useful in the detection of myocardial viability in patients with acute myocardial infarction. Furthermore, this modality is equivalent to ^{18}F-FDG-PET imaging.

REFERENCES

1. Brodie BR, Grines CL, Ivanhoe R, Knopf W, Taylor G, O'Keefe J, et al. Six-month clinical and angiographic follow-up after direct angioplasty for acute myocardial infarction. Final results from the Primary Angioplasty Registry. *Circulation* 1994; 90 (1): 156–162.
2. Serruys PW, Emanuelsson H, van der Giessen W, Lunn AC, Kiemeney F, Macaya C, et al. Heparin-coated Palmaz-Schatz stents in human coronary arteries. Early outcome of the Benestent-II Pilot Study. *Circulation* 1996; 93 (3): 412–422.
3. Almagor Y, Feld S, Kiemeneij F, Serruys PW, Morice MC, Colombo A, et al. First international new intravascular rigid-flex endovascular stent study (FINESS): clinical and angiographic results after elective and urgent stent implantation. The FINESS Trial Investigators. *J Am Coll Cardiol* 1997; 30 (4): 847–854.
4. Christian TF, Behrenbeck T, Pellikka PA, Huber KC, Chesebro JH, Gibbons RJ. Mismatch of left ventricular function and infarct size demonstrated by technetium-99m-isonitrile imaging after reperfusion therapy for acute myocardial infarction: identification of myocardial stunning and hyperkinesia. *J Am Coll Cardiol* 1990; 16: 1632–1638.
5. Grines CL, O'Neill WW, Anselmo EG, Juni JE, Topol EJ. Comparison of left ventricular function and contractile reserve after successful recanalization by thrombolysis versus rescue percutaneous transluminal coronary angioplasty for acute myocardial infarction. *Am J Cardiol* 1988; 62: 352–357.
6. Topol EJ, Weiss JL, Brinker JA, Brin KP, Gottlieb SO, Becker LC, et al. Regional wall motion improvement after coronary thrombolysis with recombinant tissue plasminogen activator: importance of coronary angioplasty. *J Am Coll Cardiol* 1985; 6 (2): 426–433.
7. Kiat H, Berman DS, Maddahi J, De Yang L, Van Train K, Rozanski A, et al. Late reversibility of tomographic myocardial thallium-201 defects: an accurate marker of myocardial viability. *J Am Coll Cardiol* 1988; 12 (6): 1456–1463.
8. Dilsizian V, Rocco TP, Freedman NMT, Leon MB, Bonow RO. Enhanced detection of ischemic but viable myocardium by the reinjection of thallium after stress-redistribution imaging. *N Engl J Med* 1990; 323: 141–146.
9. Rocco TP, Dilsizian V, McKusick KA, Fischman AJ, Boucher CA, Strauss HW. Comparison of thallium redistribution with rest reinjection imaging for the detection of viable myocardium. *Am J Cardiol* 1990; 66: 158–163.
10. Tartagni F, Fallani F, Corbelli C, Balletta A, Franchi R, Lombardi A, et al. Detecting hibernated myocardium with SPECT and thallium-glucose-insulin infusion. *J Nucl Med* 1995; 36 (8): 1377–1383.
11. Omatsu-Kanbe M, Kitasato H. Insulin stimulates the translocation of Na+/K(+)-dependent ATPase molecules from intracellular stores to the plasma membrane in frog skeletal muscle. *Biochem J* 1990; 272 (3): 727–733.
12. Hundal HS, Marette A, Mitsumoto Y, Ramlal T, Blostein R, Klip A. Insulin induces translocation of the alpha 2 and beta 1 subunits of the Na^+/K^+-ATPase from intracellular compartments to the plasma membrane in mammalian skeletal muscle. *J Biol Chem* 1922; 267: 5040–5043.
13. Gehring PJ, Hammond PB. The inter-relationship between thallium and potassium in animals. *J Pharmacol Exper Ther* 1967; 155: 197–201.
14. McCall D, Zimmer LJ, Katz AM. Kinetics of thallium exchange in metabolic factors on thallium exercise exchange in cultured rat myocardial cells. *Circ Res* 1985; 56: 370–376.
15. Takeda T, Toyama H, Hatakeyama R, Satoh M, Jin W, Ishikawa N, et al. An approach of cross talk correction by triple energy acquisition method. *Med Imag Tech* 1991; 9: 305–306.
16. Koral KF, Swailem FM, Buchbinder S, Clinthorne NH, Rogers L, Tsui BMW. SPECT dual-energy-window Compton correction: Scatter multiplier required for quantification. *J Nucl Med* 1990; 31: 90–98.
17. Zhang H, Tian M, Oriuchi N, Higuchi T, Tanada S, Endo K. Oncological diagnosis using positron coincidence gamma camera with fluorodeoxyglucose in comparison with dedicated PET. *Br J Radiol* 2002: 75: 409–416.
18. Schofer J, Mathey DG, Montz R, Bleifeld W, Stritzke P. Use of dual intracoronary scintigraphy with thallium-201

and technetium-99m pyrophosphate to predict improvement in left ventricular wall motion immediately after intracoronary thrombolysis in acute myocardial infarction. *J Am Coll Cardiol* 1983; 2: 737–744.
19. Hashimoto T, Kambara H, Fudo T, Tamaki S, Takatsu Y, Hattori R, et al. Significance of technetium-99m/thallium-201 overlap on simultaneous dual emission computed tomography in acute myocardial infarction. *Am J Cardiol* 1988; 61: 1181–1186.
20. Naruse H, Arii T, Kondo T, Morita M, Ohyanagi M, Iwasaki T, et al. Clinical usefulness of iodine 123-labeled fatty acid imaging in patients with acute myocardial infarction. *J Nucl Cardiol* 1998; 5: 275–284.
21. Abe Y, Sugiura T, Takehana K, Kamihata H, Karakawa M, Inada M, et al. Clinical significance of denervated but viable myocardium in patients with recanalized acute myocardial infarction. *Nucl Med Commun* 1999; 20: 727–735.
22. Nakajima K, Shuke N, Nitta Y, Taki J, Matsubara T, Terashima N, et al. Comparison of ^{99m}Tc-pyrophosphate, ^{201}T1 perfusion, ^{123}I-labelled methyl-branched fatty acid and sympathetic imaging in acute coronary syndrome. *Nucl Med Commun* 1995; 16: 494–503.
23. Tomoda H, Yoshioka K, Shiina Y, Tagawa R, Ide M, Suzuki Y. Regional sympathetic denervation detected by iodine-123-metaiodobenzylguanidine in non-Q-wave myocardial infarction and unstable angina. *Am Heart J* 1994; 128: 452–458.
24. Kawabata M, Morozumi K, Hujita M, Watanabe T, Kotani J, Nakayama H, et al. Freeze image of urgent Tc-tetrofosmin myocardial SPECT can evaluate area at risk of AMI. *Jpn Circ J* 1999; 62: 961.
25. Tillisch J, Brunken R, Marshall R, Schwaiger M, Mandelkern M, Phelps M, et al. Reversibility of cardiac wall motion abnormalities predicted by positron tomography. *N Engl J Med* 1986; 314: 884–888.
26. Tamaki N, Yonekura Y, Yamashita K, Saji H, Magata Y, Senda M, et al. Positron emission tomography using fluorine-18 deoxyglucose in evaluation of coronary artery bypass grafting. *Am J Cardiol* 1989; 64 (14): 860–865.
27. Marwick TH, Nemec JJ, Lafont A, Salcedo EE, Macintyre WJ. Prediction improvement in exercise capacity after revascularization. *Am J Cardiol* 1992; 69: 854–859.
28. Sebree L, Bianco JA, Subramanian R, Wilson MA, Swanson D, Hegge J, et al. Discordance between accumulation of C-14 deoxyglucose and Tl-201 in reperfused myocardium. *J Mol Cell Cardiol* 1991; 23: 603–616.
29. Nonogi H, Miyazaki S, Goto Y, Ishida Y, Uehara T, Nishimura T. Efficacy and limitation of F-18-fluorodeoxyglucose positron emission tomography during fasting to assess myocardial viability in the acute phase of myocardial infarction. *Internal Medicine* 1998; 37: 653–661.
30. Okumura W, Iwasaki T, Toyama T, Kurabayashi M, Suzuki T, Inoue T, et al. ^{18}F-FDG PET imaging may overestimate myocardial viability in acute myocardial infarction: Microautoradiographic and immunohistochemical study. *Jpn Circ J* 2001; 65: 229.
31. Chiba H, Kusuoka H, Ohno J, Nishimura T. Glucose-loading thallium-201 myocardial SPECT. *J Nucl Med* 1997; 38: 573–577.
32. Krivokapich J, Shine KI. Effects of hyperkalemia and glycoside on ^{201}Tl exchange in rabbit ventricle. *Am J Physiol* 1981; 240: H612–H616.
33. L'Abbate A, Biagini A, Michelassi C, Maseri A. Myocardial kinetics of ^{201}Tl and potassium in man. *Circulation* 1979; 60: 776–782.
34. Zierler KL. Effects of insulin on potassium efflux from rat muscle in the presence and absence of glucose. *Am J Physiol* 1968; 1066–1070.
35. Rogers WJ, Russell RO, McDaniel HG, Rockley CR. Acute effects of glucose-insulin-potassium infusion on myocardial substrates, coronary blood flow and oxygen consumption in man. *Am J Cardiol* 1977; 40: 421–428.
36. Runnman EM, Lamp ST, Weiss JN. Enhanced utilization of exogenous glucose improves cardiac function in hypoxic rabbit ventricle without increasing total glycolytic flux. *J Clin Inverst* 1990; 86: 1222–1233.
37. De Sutter J, De Winter F, Van de Wiele C, De Bondt P, D'Asseler Y, Dierckx R. Cardiac fluorine-18 fluorodeoxyglucose imaging using a dual-head gamma camera with coincidence detection: a clinical pilot study. *Eur J Nucl Med* 2000; 27: 676–685.
38. Toyama T, Hoshizaki H, Isobe N, Adachi H, Naito S, Oshima S, et al. Detecting viable hibernating myocardium in chronic coronary artery disease—A comparison of resting ^{201}Tl single photon emission computed tomography (SPECT), ^{99m}Tc-methoxy-isobutyl isonitrile SPECT after nitrate administration, and ^{201}Tl SPECT after ^{201}Tl-glucose-insulin infusion. *Jpn Circ J* 2000; 64: 937–942.